JOURNAL OF GEOPHYSICAL RESEARCH, VOL. 115, D03206, doi:10.1029/2009JD012630, 2010

Ion-mediated nucleation in the atmosphere: Key controlling parameters, implications, and look-up table

Fangqun Yu[1]

Received 10 June 2009; accepted 18 September 2009; published 13 February 2010.

[1] Nucleation is an important source of atmospheric particles and ubiquitous ions in the atmosphere have long been known to promote nucleation. An ion-mediated nucleation (IMN) mechanism based on a kinetic model is supported by recent measurements of the excess charge on freshly nucleated particles and ion cluster evolution during nucleation events. Here we investigate the dependence of steady state IMN rate (J_{IMN}) on key controlling parameters. We find that sulfuric acid vapor concentration, temperature, relative humidity, ionization rate, and surface area of preexisting particles have profound and nonlinear impacts on J_{IMN}. The sensitivities of J_{IMN} to the changes in these key parameters may imply important physical feedback mechanisms involving climate and emission changes, solar variations, nucleation, aerosol number abundance, and aerosol indirect radiative forcing. We also describe a five-dimensional J_{IMN} look-up table derived from the most recent version of the IMN model, with the key parameters covering a wide range of atmospheric conditions. With the look-up table and a multiple-variable interpolation subroutine, J_{IMN} and the properties of critical clusters can be determined efficiently and accurately under given atmospheric conditions. The look-up table reduces the computational costs of the IMN rate calculations significantly (by a factor of around 8000) and can be readily incorporated into multidimensional models to study the secondary particle formation via IMN and associated climatic and health effects.

Citation: Yu, F. (2010), Ion-mediated nucleation in the atmosphere: Key controlling parameters, implications, and look-up table, *J. Geophys. Res.*, *115*, D03206, doi:10.1029/2009JD012630.

1. Introduction

[2] The magnitude of the aerosol indirect radiative forcing is poorly constrained in climate models, and this is the dominant uncertainty in assessing climate change [*Intergovernmental Panel on Climate Change*, 2007]. The aerosol indirect radiative forcing is largely determined by the number abundance of particles that can act as cloud condensation nuclei (CCN) [e.g., *Twomey*, 1977; *Albrecht*, 1989]. New particle formation, which has been frequently observed throughout the troposphere [*Kulmala et al.*, 2004a; *Yu et al.*, 2008], is an important source of atmospheric CCN. To accurately assess the influences of aerosols on climate, interpret past climate, and project future changes, the contribution of secondary particle formation and growth to CCN abundance have to be understood and properly incorporated in the large-scale models. In this regard, it is critical to achieve a clear physical understanding of atmospheric particle nucleation mechanisms, especially the dependence of nucleation rates on key atmospheric parameters.

[3] Based on an up-to-date kinetically consistent ion-mediated nucleation model (IMN) incorporating recently available thermodynamic data and schemes, *Yu* [2006] showed that ions can lead to significant particle formation not only in the upper troposphere but also in the lower troposphere (including boundary layer). The involvement of ions in many boundary layer nucleation events has been confirmed by measurements of the evolution of charged clusters during nucleation events and the observed overcharge of freshly nucleated nanometer-sized particles [*Iida et al.*, 2006; *Hirsikko et al.*, 2007; *Laakso et al.*, 2007; *Gagné et al.*, 2008]. Both 3 year records of ion mobility measurements [*Hirsikko et al.*, 2007] and 1 year overcharging ratio measurements for freshly nucleated particles [*Gagné et al.*, 2008] indicate that ions are involved in more than 90% of the particle formation events that can be clearly identified, although the relative contribution of ion and neutral nucleation remains controversial (see section 2.2 for more discussion on this). Detailed case studies [*Yu and Turco*, 2008] indicate that for most of well-defined nucleation events observed in Hyytiälä, Finland, the predictions based on the ion-mediated nucleation (IMN) model are in good agreement with field data for a range of variables, including critical nucleation sizes, size-dependent overcharging ratios, and the concentrations of 1.8–3 nm stable clusters and 3–6 nm particles, as well as their diurnal variations. Thus, we have experimental evidence that IMN may be important in the atmosphere.

[4] In this paper we study the dependence of IMN rates on key parameters and derive an IMN look-up table from the detailed kinetic IMN model. An overview of the IMN

[1]Atmospheric Sciences Research Center, State University of New York at Albany, Albany, New York, USA.

0148-0227/10/2009JD012630$09.00

mechanism is given in section 2. The dependence of IMN rates on key parameters and associated implications are discussed in section 3. Section 4 describes the IMN look-up table, which can be used for a quick and accurate calculation of IMN rates at given conditions. Last, section 5 is the summary.

2. Overview of Ion-Mediated Nucleation Mechanism

2.1. Kinetic IMN Model: Physics, Features, and Recent Development

[5] Ions, which are generated continuously and ubiquitously in the atmosphere by cosmic radiation and radioactive decay, have long been suggested to promote nucleation [*Castleman et al.*, 1978; *Arnold*, 1980; *Chan and Mohnen*, 1980; *Hamill et al.*, 1982; *Raes et al.*, 1986]. *Yu and Turco* [1997, 2000, 2001] developed a comprehensive approach for studying nucleation processes involving ion clusters. They utilized a kinetic model that explicitly treats the complex interactions among small air ions, neutral and charged clusters of various sizes, precursor vapor molecules, and preexisting aerosols. Compared to homogeneous nucleation, which involves the formation of small, transient neutral molecular clusters, nucleation onto ions is favored because: (1) small charged clusters are typically much more stable thermodynamically than their neutral counterparts [*Yu*, 2005, 2006], (2) the initial growth rates of small ion clusters are enhanced by the dipole-charge interaction between the core ion and the strongly dipolar condensing molecules [*Nadykto and Yu*, 2003], and (3) there is a continuous and ubiquitous supply of stable, fast growing ionic embryos. *Yu and Turco* [2000] refer to the coupled formation and evolution of cluster size distributions, including both charged and neutral clusters, under the influence of ionization, recombination, neutralization, condensation, evaporation, coagulation, and scavenging as IMN.

[6] The IMN theory differs substantially from classical ion-nucleation theory, which is commonly adopted in the literature [e.g., *Hamill et al.*, 1982; *Raes et al.*, 1986; *Laakso et al.*, 2002]. Classical "ion nucleation" is based on a simple modification of the free energy associated with the formation of a "critical nucleation embryo" in which the electrostatic potential energy induced by the embedded charge is included. However, this classical approach does not properly account for the kinetic limitation to embryo development imposed by the typically low atmospheric concentrations of precursors, especially sulfuric acid. In addition, the important contribution of neutral clusters resulting from ion-ion recombination to nucleation is not considered in the classical ion nucleation theory. By contrast, in IMN theory, the kinetic effect of charge on cluster growth rates and the contribution of neutral clusters resulting from the neutralization of charged clusters are explicitly considered.

[7] IMN explains the rapid initial growth of small clusters, as a result of the charge-neutral interactions. This initial growth phase (to sizes of $\sim$1.5 nm diameter) is not to be confused with later stages of stable nanoparticle growth (from $\sim$2–3 nm and larger). In the initial phase, ion-molecule interactions greatly accelerate the kinetics of molecular association, by up to an order of magnitude. However, by the time the nucleating embryos are larger than $\sim$1.5 nm in diameter, the charge-enhanced growth effect becomes quite small due to the inverse relationship between charge effect and embryo size [*Nadykto and Yu*, 2003] and rapid neutralization of ion embryos [*Yu*, 2006; *Yu and Turco*, 2008]. Subsequently, the growth rate is dominated by the vapor pressure of the major condensing species. In the case of organic condensates, for example, the normal Kelvin effect would predict that the growth rate accelerates as the particle size increases, opposite to the effect produced by a fixed particle charge. This predicted pattern of growth is consistent with observations [e.g., *Kulmala et al.*, 2004b].

[8] Built upon an earlier version of the IMN model [*Yu and Turco*, 1997, 2000, 2001], *Yu* [2006] developed a second-generation IMN model which incorporates new thermodynamic data [*Froyd*, 2002; *Wilhelm et al.*, 2004] and physical algorithms [*Nadykto and Yu*, 2003; *Yu*, 2005] and explicitly treats the evaporation of neutral and charged clusters. The uncertainty in the IMN model has been further reduced by using two independent measurements to constrain monomer hydration in the H_2SO_4-H_2O system, and by incorporating recently determined energetics of small neutral H_2SO_4-H_2O clusters [*Yu*, 2007]. It should be pointed out that the present IMN model is for the H_2SO_4-H_2O binary system. In the atmosphere, species other than H_2SO_4 and H_2O (such as NH_3, amines, HNO_3, and some organics) may be involved in the IMN process under some conditions. Obtaining necessary thermodynamic data and extending the IMN model for a multiple-component nucleation system will be the subject of future research.

[9] Based on the most comprehensive and well-constrained case studies of atmospheric nucleation processes to date (at least to our knowledge), *Yu and Turco* [2008] concluded that beyond a reasonable level of uncertainty, IMN appears to be the dominant nucleation mechanism in at least a large fraction of nucleation events observed during an intensive field campaign in boreal forests. In addition, the global nucleation spatial patterns and absolute magnitude predicted using the IMN mechanism is reasonably consistent to land-, ship-, and aircraft-based observations [*Yu et al.*, 2008]. More recently, *Yu and Luo* [2009] used global size resolved aerosol microphysics modeling to show that IMN is able to account for (within a factor of 2) the annual mean particle number concentrations observed in many parts of troposphere.

2.2. Controversy With Regard to the Importance of IMN in the Atmosphere

[10] While our analyses indicate that the ion mobility data and the measurements of excess charge on freshly nucleated particles in the boreal forest support the dominance of the IMN mechanism [*Yu and Turco*, 2007, 2008], Kulmala and colleagues [*Laakso et al.*, 2007; *Kulmala et al.*, 2007; *Gagné et al.*, 2008; *Boy et al.*, 2008; *Manninen et al.*, 2009] concluded that, based on their analysis of the same data set, IMN contributes only up to $\sim$10% to the boreal forest nucleation. Given such discrepancies, we discuss these studies here along with possible reasons for the differences.

[11] Kulmala and colleagues' studies concluding the dominance of neutral nucleation process include the following: (1) *Laakso et al.* [2007] and *Gagné et al.* [2008] extrapolated measured charging states of nucleation mode

particles (~3–7 nm) down to smaller sizes (1–2 nm) and concluded that the contribution of IMN to total nucleation rate was either negligible or relatively small in a large fraction of days considered. (2) *Kulmala et al.* [2007] and *Manninen et al.* [2009] calculated the formation rate of total and charged 2 nm particles from the particle concentrations detected in the size range of ~2–3 nm, and concluded that IMN contributes ~10% to the boreal forest new particle formation events. (3) *Boy et al.* [2008] simulated 4 days of nucleation events using atmospheric input data from the SMEAR II station. They calculated the IMN rate based on the model of *Kazil and Lovejoy* [2007], and used the empirical activation ($J_{act} = A\ [H_2SO_4]$) and kinetic nucleation formulas ($J_{kin} = K\ [H_2SO_4]^2$) to represent neutral nucleation. By comparing their calculated ion and neutral nucleation rates, *Boy et al.* [2008] concluded that IMN contributes between <0.5 to 12% to the total number of particles nucleated inside the mixed layer in the boreal forests.

[12] *Yu and Turco*'s [2007, 2008] studies pointing out the dominance of the IMN process include the following: (1) *Yu and Turco* [2007] showed, based on a conservative analytical analysis of the neutralization of charged particles, that the observed charging states of nucleated particles (~3–7 nm) reported by *Laakso et al.* [2007] are fully consistent with the dominance of IMN in most of the nucleation events. (2) Based on the well-constrained case studies of nucleation events characterized in Hyytiälä, with a kinetic nucleation model accounting for the size-dependent microphysics of neutral and charged clusters, *Yu and Turco* [2008] demonstrated a good agreement between the IMN predictions and field data for a wide range of the key parameters including the overcharging ratio (OR) of 3–7 nm particles and concluded that IMN is likely to be the dominant nucleation mechanism in at least a large fraction of nucleation events in boreal forests.

[13] One possible cause of such different conclusions is that Kulmala and colleagues' analyses focused on 2–3 nm particles while Yu and Turco's kinetic modeling considered the actual dynamics of the formation of clusters with diameters ranging from ~0.5 nm to >3 nm. Kulmala and colleagues assume that all neutral particles ~2 nm or growing into 2 nm are from neutral nucleation. This may lead to significant underestimation of the IMN contribution because a significant fraction of neutral particles ~2 nm and smaller may be formed from the IMN [*Yu and Turco*, 2008]. *Yu et al.* [2007] have demonstrated that *Laakso et al.*'s [2007] conclusion that IMN has a negligible or small contribution to new particle formation is inconsistent with their own analysis of the charging state (Sc) of 1 nm particles. *Laakso et al.*'s [2007] conclusion appears to be based on Sc values of 2 nm particles. However, it is more appropriate to use Sc at 1 nm because neutral particles at 1–2 nm may actually be produced by the neutralization of particles formed on ions and thus are a direct result of IMN [*Yu and Turco*, 2008]. Based on Sc at 1 nm given by *Laakso et al.* [2007], a large fraction (60%) of the days have either a significant or dominant (Sc > 50) contribution from IMN, while only a small fraction (13%) of days have either negligible (Sc < 1) or small (Sc < 10) contributions from IMN [*Yu et al.*, 2007]. These considerations lead us to conclude that Laakso et al.'s analysis may actually support Yu and Turco's conclusion. Similarly, we think that *Kulmala et al.* [2007] and *Manninen et al.* [2009] underestimated the importance of IMN because they assumed all neutral particles growing to ~2 nm were produced via neutral nucleation, while in the reality these particles may have been formed via the neutralization of particles formed on ions. The conclusion of *Boy et al.* [2008] is not surprising because they used the ion nucleation model similar to that of *Lovejoy et al.* [2004], which underpredicts ion nucleation rate by several orders of magnitude [*Yu and Turco*, 2008]. In addition, *Boy et al.* [2008] used empirical activation and kinetic nucleation formulas to represent neutral nucleation. It remains to be established whether the empirical formula indicates a new nucleation mechanism or if it simply represents an empirical fitting of exiting nucleation process such as IMN [*Yu and Turco*, 2008].

[14] While more comprehensive studies are needed in order to more clearly resolve the IMN controversy, our analyses given above indicate that Kulmala and colleagues might have underestimated the importance of IMN, and the results of *Laakso et al.* [2007] may actually support the significance of IMN. It should be emphasized that the dominance of the neutral nucleation process will lead to the undercharging of freshly nucleated particles. *Laakso et al.* [2007] and *Gagné et al.* [2008] showed that ion-DMPS detected substantial undercharging of freshly nucleated particles in only ~10% of nucleation event days. The undercharging could be an indication of the dominance of neutral nucleation; however it may also be a result of air mass inhomogeneity and uncertainties in measurements [*Yu and Turco*, 2008].

3. Dependence of IMN Rates on Key Parameters and Implications

[15] The IMN model explicitly solves the dynamic equations governing the size distribution evolution of neutral, positively charged, and negatively charged cluster/particles. The IMN rates (denoted as J_{IMN}) are calculated based on the net fluxes of particles across the critical size of neutral embryos. Under a given condition, cluster distribution and nucleation rate reach steady state after a certain amount of time. Detailed information about the IMN model and how IMN rates are determined is given by *Yu* [2006]. All the IMN rates presented in this paper are the steady state values, and the steady state apparent IMN rates across the clusters containing 10 sulfuric molecules (dry diameter around 1.2 nm) are used for the conditions that give very small critical size (containing less than 10 sulfuric molecules). The current version of the IMN model only considers the binary H_2SO_4-H_2O system, and there are five key parameters controlling J_{IMN}: sulfuric acid vapor concentration ($[H_2SO_4]$), temperature (T), relative humidity (RH), ionization rate (Q), and surface area of preexisting particles (S). Figures 1–5 show the dependence of J_{IMN} on these parameters, based on the calculations from full IMN model (solid lines) and IMN look-up table detailed in section 4 (dashed lines).

3.1. Sulfuric Acid Vapor Concentration ($[H_2SO_4]$)

[16] Figure 1 gives J_{IMN} as a function of $[H_2SO_4]$ for four different atmospheric states. There is no doubt that $[H_2SO_4]$ is a key parameter controlling J_{IMN}. To achieve a nucleation

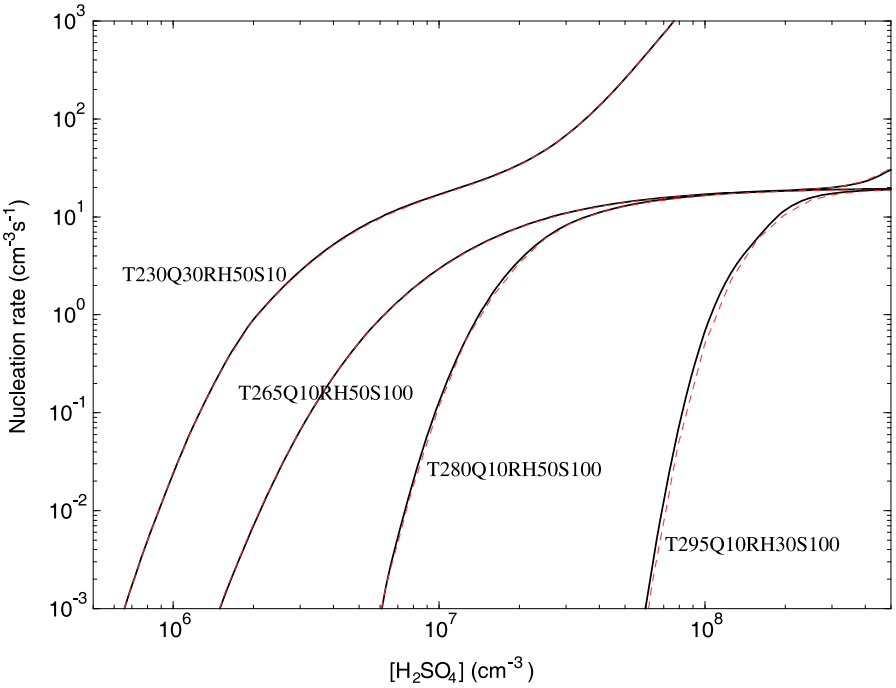

Figure 1. Ion-mediated nucleation rate as a function of sulfuric acid vapor concentration ($[H_2SO_4]$) under four different ambient conditions, calculated with the full IMN model (solid lines) and IMN look-up table (dashed lines). In the legend, read T295Q10RH50S100 as T = 295K, Q = 10 ion pairs $cm^{-3}s^{-1}$, RH = 50%, and S = 100 μm^2 cm^{-3}.

rate of 1 $cm^{-3}s^{-1}$ under typical values of Q (10 ion pairs $cm^{-3}s^{-1}$), RH (50%), and S (100 μm^2 cm^{-3}), $[H_2SO_4]$ has to be around 6×10^6, 9×10^6, 2.5×10^7, and 10^8 cm^{-3} for T = 265, 275, 285, and 295 K, respectively. Nucleation events have been frequently observed in boreal forests during the spring season when T is ~270–285 K and peak $[H_2SO_4]$ is in the range of $5 \times 10^6 - 3 \times 10^7$ cm^{-3}. It has been shown by *Yu and Turco* [2008] that the IMN mechanism appears to be able to account for at least a large fraction of these nucleation events and is supported by the observed overcharging of freshly nucleated particles.

[17] Under the conditions considered in Figure 1, J_{IMN} is very sensitive to $[H_2SO_4]$ when $[H_2SO_4]$ is relatively low and J_{IMN} is relatively small, and becomes insensitive at higher $[H_2SO_4]$, because of the limitation of nucleation by ionization rate. For low T, J_{IMN} becomes sensitive to $[H_2SO_4]$ when $[H_2SO_4]$ is high (for example, see the curve with T = 230 K when $[H_2SO_4] > \sim 2 \times 10^7/cm^3$) because of the dominance of binary homogeneous nucleation (BHN) under such conditions. It should be noted that BHN is an integrated part of IMN [*Yu*, 2006].

[18] The importance of $[H_2SO_4]$ in controlling J_{IMN} can also be seen from the global spatial distribution of J_{IMN} presented by *Yu et al.* [2008], showing that high-nucleation zones are generally confined to high sulfur source regions. The sensitivity of J_{IMN} to $[H_2SO_4]$ implies that future changes in anthropogenic and natural emissions of sulfur species may have important impacts on new particle formation, aerosol abundance, and radiative forcing. For example, *Charlson et al.* [1987] proposed that a warmer climate would increase dimethylsulphide (DMS) emissions which in turn leads to higher formation rates of sulfate aerosols and CCN abundance. The resulting increase in cloud albedo should reflect more sunlight back to space and thus cool the Earth. On the other hand, the pollution controlling strategies aimed to reduce anthropogenic sulfur emissions may significantly decrease aerosol number abundance in the atmosphere and thus diminish the cooling effects of atmospheric aerosols.

3.2. Temperature

[19] Figure 2 illustrates the dependence of J_{IMN} on temperature (T) under four different ambient conditions. Similar to $[H_2SO_4]$, T has a strong effect on J_{IMN}. Under a variety of conditions given in Figure 2, J_{IMN} is very sensitive to T when J_{IMN} increases from insignificant ($<\sim 0.01$ $cm^{-3}s^{-1}$) to significant ($>\sim 1$ $cm^{-3}s^{-1}$) as T decreases. After J_{IMN} reaches a significant level, further decreases of T (with other parameters fixed) have relatively small effects because nucleation under such conditions is limited by ionization rates. When T is very low, BHN becomes dominant and the nucleation rates become sensitive to T again. Under typical values of Q (10 ion pairs $cm^{-3}s^{-1}$), RH(50%), and S (100 μm^2 cm^{-3}), to achieve a nucleation rate of 1 $cm^{-3}s^{-1}$, T should be around 268, 277, 286, and 291 K, for $[H_2SO_4] = 5 \times 10^6$, 10^7, 3×10^7, and 6×10^7 cm^{-3}, respectively. Clearly, much higher $[H_2SO_4]$ is needed to achieve a similar level of nucleation rate at higher temperature.

[20] Based on mass-resolved ion cluster distributions measured in the summer of 2002 at an urban site in Atlanta, Georgia, and in the late summer/fall of 2004 at the National Center for Atmospheric Research (NCAR) Marshall Field Site, *Eisele et al.* [2006] concluded that ion-induced nucleation was unlikely to have contributed significantly to the

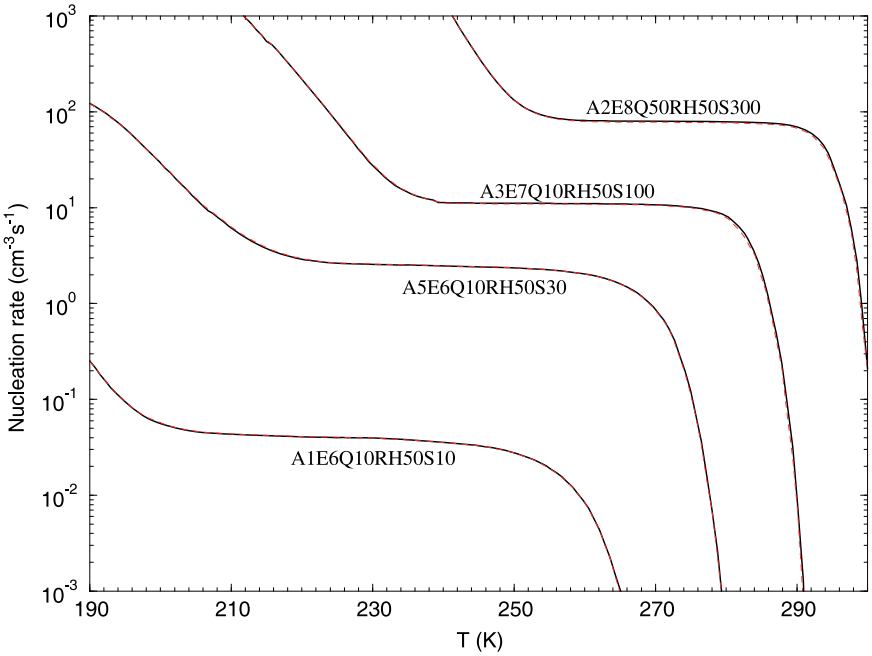

Figure 2. The dependence of predicted ion-mediated nucleation rate on T for four different ambient conditions, based on the full IMN model (solid lines) and IMN look-up table (dashed lines). In the legend, read A3E7Q10RH50S100 as $[H_2SO_4] = 3 \times 10^7 cm^{-3}$, Q = 10 ion pairs $cm^{-3}s^{-1}$, RH = 50%, and S = 100 μm^2 cm^{-3}.

new particle formation observed on some days during the study period. Under the atmospheric conditions corresponding to the days that *Eisele et al.*'s [2006] measurements were made (T > ~290 K, RH < ~ 40%, $[H_2SO_4] < \sim 3 \times 10^7$ cm^{-3}), the IMN model would likewise predict a negligible rate of nucleation ($<10^{-3}$ $cm^{-3}s^{-1}$; see Figure 2). Thus, the IMN mechanism does not directly conflict with these measurements. It is possible that additional species may be involved and enhance nucleation in urban and other disturbed environments. By analyzing the charged fractions (CFs) of 3–5.5 nm particles measured at NCAR's Marshall Field Site, *Iida et al.* [2006] concluded that while obviously involved in nucleation on some days, ions overall contributed insignificantly to new particle formation observed at the site. Our model predicts negligible IMN rates on days with high temperature (>~290 K). However, the model also suggests that IMN can become significant during periods of relatively lower temperatures (<~285 K). *Iida et al.* [2006] derived their CFs at 1 nm by extrapolating from observed CFs for 3–5.5 nm particles, and the interpretive analysis is likely subject to large uncertainties. For example, during a nucleation period on 1 June 2004, the 3–5.5 nm particles were clearly overcharged, with ORs above 2 [*Iida et al.*, 2006]. Based on our size-dependent kinetic modeling, an OR above 2 for 3–5 nm particles should indicate the dominance of IMN [*Yu and Turco*, 2008], whereas *Iida et al.* [2006] inferred that IMN only contributed ~0.4% of the nucleation. A more detailed case study of measurements reported by *Iida et al.* [2006] may shed new light on the mechanisms of particle nucleation.

[21] In the atmosphere, nucleation events typically last for several hours only and there exist clear seasonal variations in the frequency of nucleation events. According to IMN mechanism, temperature and $[H_2SO_4]$ are the two most important factors controlling the start and end of nucleation events, although other parameters also contribute to the changes in nucleation rates. The optimum conditions for IMN are relatively high $[H_2SO_4]$ and relatively low T, which may explain (at least partially) why nucleation generally occurs in the morning and why nucleation event frequency peaks in the spring and fall [e.g., *Stanier et al.*, 2004; *Laaksonen et al.*, 2008].

[22] Figure 2 shows that, within the T range that J_{IMN} changes from insignificant (<~0.01 $cm^{-3}s^{-1}$) to significant (>~1 $cm^{-3}s^{-1}$), a 2 K difference in T causes up to around 1 order of magnitude difference in J_{IMN}. Such high sensitivity of J_{IMN} to temperature may have important implications. For example, future global warming may significantly suppress new particle formation in the atmosphere, reduce CCN abundance and aerosol indirect radiative cooling, and thus may imply a positive climate/nucleation feedback mechanism. The magnitude of this new positive feedback mechanism proposed here should be assessed with global climate models that incorporate the IMN mechanism and proper size-resolved aerosol microphysics.

[23] It is also clear from Figure 2 that at a constant level of $[H_2SO_4]$, nucleation is more favored in air with slightly lower temperature. One example is that under some conditions, nucleation is favored in the top of boundary layer instead of surface because of the temperature difference. Actually, many of the nucleation events observed at the surface may be associated with the mixing of particles nucleated aloft (especially particle size distribution evolutions exhibiting the "apple" shape rather than the "banana" shape [*Yu et al.*, 2008]). The high sensitivity of J_{IMN} to T may also imply large inhomogeneities in nucleation rates due

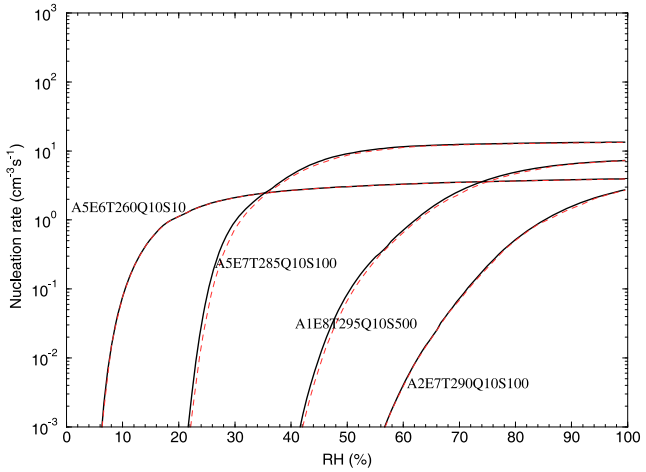

Figure 3. The dependence of predicted IMN rate on RH under four selected conditions, based on the full IMN model (solid lines) and IMN look-up table (dashed lines). In the legend, read A1E7T275Q10S50 as $[H_2SO_4]$ = 3 × 10^7cm^{-3}, Q = 10 ion pairs cm^{-3}s^{-1}, T = 275 K, and S = 50 μm^2 cm^{-3}.

to temperature fluctuation in different air masses. Airborne measurements of nucleation-mode aerosol concentrations over boreal forests reveal significant variability in nucleated particle concentrations attributable to variability in land coverage between forests and lakes [*O'Dowd et al.*, 2008], and temperature difference could be one of the factors contributing to the variability.

3.3. Relative Humidity

[24] The effects of relative humidity (RH) on J_{IMN} under four atmospheric conditions are shown in Figure 3. With all other parameters fixed, J_{IMN} increases with increasing RH until J_{IMN} reaches a level that is limited by ionization rates. The effect of RH on J_{IMN} can be very significant under some conditions. For example, J_{IMN} increases by about 3 orders of magnitude when RH increases (1) from 60% to 90% under one shown condition (T = 290 K, $[H_2SO_4] = 2 \times 10^7$cm^{-3}, Q = 10 ion pairs cm^{-3}s^{-1}, and S = 100 μm^2 cm^{-3}) and (2) from 20% to 30% under another condition (T = 285 K, $[H_2SO_4] = 5 \times 10^7$cm^{-3}, Q = 10 ion pairs cm^{-3}s^{-1}, and S = 100 μm^2 cm^{-3}).

[25] In the real atmosphere, RH has clear diurnal variations which are associated with T changes. The increase of temperature generally leads to the decrease of RH which in turn enhances the effect of T on nucleation rates. *Yu and Turco* [2008] showed in the well-constrained case studies that the increase in T and decrease in RH are the main reasons for the shut-off of nucleation events around noontime observed in boreal forests.

[26] Most climate models predict little change in global RH as a result of projected global warming associated with greenhouse effect. Nevertheless, some observations and modeling analysis indicate that RH may decrease as T increases, especially in the middle and upper troposphere [*Minschwaner and Dessler*, 2004]. For each degree of surface warming, absolute RH could decrease 3–5% in the upper troposphere and 3–10% in the middle troposphere [*Minschwaner and Dessler*, 2004]. The possible decrease in RH associated with global warming could further inhibit the nucleation and thus enhance the positive climate/nucleation feedback mechanism proposed above in section 3.2.

[27] It should be noted that RH variations may lead to changes in the surface area of preexisting particles which is also one of the parameters controlling nucleation rates. Due to the uptake of water by aerosols, an increase in RH will generally increase the size and hence surface area of preexisting particles, reducing nucleation rates (see section 3.5 for details). The effect of RH on particle size depends on the composition of particles. To properly assess the combined effects of RH changes on nucleation, a size- and composition-resolved aerosol microphysics model is needed.

3.4. Ionization Rate

[28] The dependence of J_{IMN} on ion production rate is presented in Figure 4 for a number of atmospheric conditions. J_{IMN} is sensitive (almost proportional) to ionization rate (Q) when $[H_2SO_4]$ is large and Q is relatively low. J_{IMN} generally increases with Q when $[H_2SO_4]$ is above around 10^7cm^{-3}. However, J_{IMN} decreases with increasing Q when Q is relatively big and $[H_2SO_4]$ is low ($<\sim 5 \times 10^6$cm^{-3}). The nonlinear dependence of J_{IMN} on Q is a result of the competition between the time needed to grow ion clusters to a stable size (t_g) and the neutralization time (t_n) of charged clusters. The neutralization by ion-ion recombination will cause the growing charged clusters to lose their growth advantage and the resulting neutral clusters may dissociate if smaller than the critical size [*Yu*, 2006]. The t_g is inversely proportional to $[H_2SO_4]$ while t_n is inversely proportional to the concentration of small opposite ions ([ion]), which is directly related to Q.

[29] The steady state J_{IMN} is limited by the local ionization rate except under the conditions that BHN becomes dominant. Ambient ions are continuously generated by galactic cosmic rays at the rate of ~2 ion pairs cm^{-3}s^{-1} at Earth's surface and up to ~20–30 ion pairs cm^{-3}s^{-1} in the upper troposphere. Other localized sources (such as radioactive emanations, corona discharge, combustion, lightning, nuclear waste, etc.) can also generate ions. Owing to natural radioactivity from soils, the ionization rate in the continental surface layer can reach up to ~10 ion pairs cm^{-3}s^{-1} [*Reiter*, 1992]. Some measurements indicate that ionization rates near the surface can exceed 100 ion pairs cm^{-3}s^{-1} due to the accumulation of radon gas in the nocturnal boundary layer [*Dhanorkar and Kamra*, 1994]. *Vartiainen et al.* [2007] detected exceptionally high ion production rates of up to 30 ion pairs cm^{-3}s^{-1} during some measurement periods. In urban zones, corona discharge may generate high concentrations of small ions as well. Small ion concentrations of up to 10^4–10^5 cm^{-3} have been observed near and downwind of high-voltage transmission lines [*Carter and Johnson*, 1988; *Suda and Sunaga*, 1990]. Under favorable conditions, these localized ion sources may lead to the formation of large concentrations of ultrafine particles. In situ measurements indicate that $[H_2SO_4]$ can reach as high as 2 × 10^8 cm^{-3} in Atlanta, Georgia [*McMurry et al.*, 2005]. Higher ion production rates coupled with higher $[H_2SO_4]$ can lead to significant nucleation, even when the concentration of preexisting particles is very high (see the top curve in Figure 4).

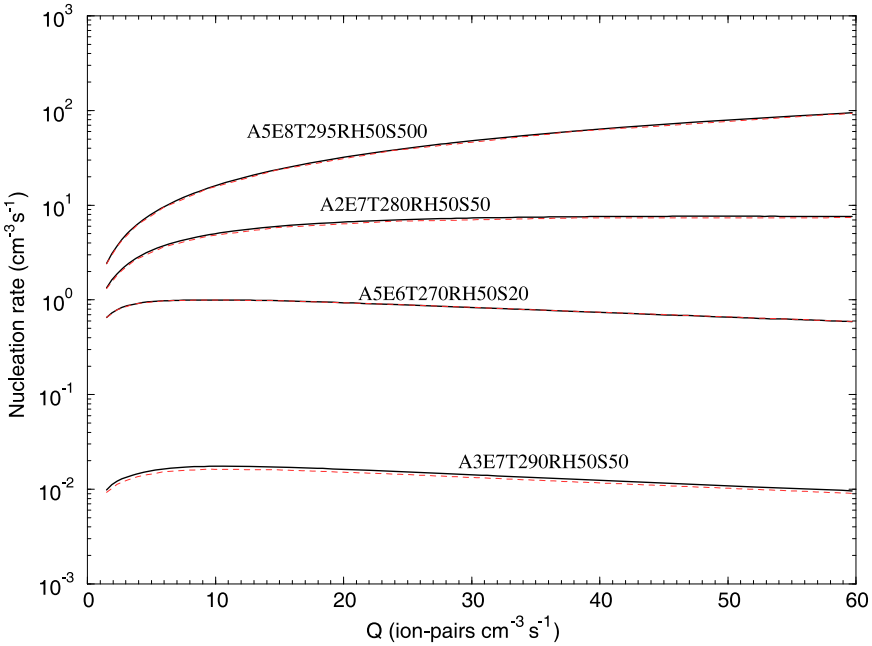

Figure 4. The dependence of predicted IMN rates on Q under four selected conditions, based on the full IMN model (solid lines) and IMN look-up table (dashed lines). In the legend, read A1E7T275RH50S50 as $[H_2SO_4] = 3 \times 10^7 cm^{-3}$, Q = 10 ion pairs $cm^{-3}s^{-1}$, T = 275 K, RH = 50%, and S = 50 μm^2 cm^{-3}.

[30] The effect of ionization rate on aerosol production in the troposphere may have important implications to the possible mechanisms amplifying the impact of solar variations on Earth's climate [*Yu*, 2002]. During a solar cycle, the values of Q vary by ~20–25% in the upper troposphere and ~5–10% in the lower troposphere at high latitudes, and by ~4–7% in the upper troposphere and ~3–5% in the lower troposphere at low latitudes [*Ney*, 1959]. Such variations in GCR-induced ionization rate associated with solar activities will cause substantial systematic changes in IMN rates which may have important climatic effects [*Yu*, 2002]. The physically based IMN mechanism presented in this paper can be applied in global aerosol models to study how solar variations may influence the abundance of climatic effective aerosols. The IMN mechanism can also be applied to study how emission of radioactive species associated with civil and military nuclear activity may affect the atmospheric ionization (especially near the source regions) and thus the new particle formation rate.

3.5. Surface Area of Preexisting Particles

[31] Figure 5 shows the dependence of steady state IMN rates on the surface area of the preexisting particles (S) under four ambient conditions. When $[H_2SO_4]$ is fixed, preexisting particles affect the nucleation by scavenging small ions and precritical clusters. The magnitude of the effect depends on the time needed to grow the molecular clusters to critical clusters (t_g) and the lifetime of these clusters due to scavenging by preexisting particles (t_s). Therefore, the effect of preexisting particles on J_{IMN} depends not only on concentration or surface area of preexisting particles, but also on the sizes of critical clusters (controlled by $[H_2SO_4]$, T, and RH) and growth rates of precritical clusters (determined mainly by $[H_2SO_4]$ and to a lesser degree by T and RH). Due to the scavenging, apparent J_{IMN} (i.e., nucleation rate calculated at particle sizes larger than critical sizes, for example 3 nm) decreases with increasing sizes where the apparent nucleation rates are calculated. As mentioned earlier, we use the steady state apparent IMN rates across the clusters containing 10 sulfuric molecules (dry diameter around 1.2 nm) for the conditions that give very small critical size (containing less than 10 sulfuric molecules).

[32] It should be noted that the effects of preexisting particle surface area on atmospheric particle formation rates should be stronger than those shown in Figure 5 for two reasons: (1) preexisting particles have a significant effect on $[H_2SO_4]$ to which the nucleation rate is very sensitive, and (2) observed particles are generally larger than 3 nm, and the scavenging of clusters/particles smaller than 3 nm but larger than critical sizes will enhance the effect of S. One implication of the effect of S on nucleation is that the emission controlling strategy aimed to reduce particulate mass (and thus surface area) may lead to the increase in new particle formation and thus particle number concentration.

[33] An additional point to note from Figure 5 is that nucleation rate can still be very high even when S > 500 μm^2 cm^{-3} in polluted areas as long as $[H_2SO_4]$ is high enough (>~10^8 cm^{-3}). Measurements indicate that $[H_2SO_4]$ can reach above $10^8 cm^{-3}$ in polluted urban areas [*McMurry et al.*, 2005]. This may explain why nucleation rates can still happen in some highly polluted regions.

4. IMN Look-Up Table

[34] In order to study aerosol nucleation in the context of three-dimensional models, the nucleation calculations must

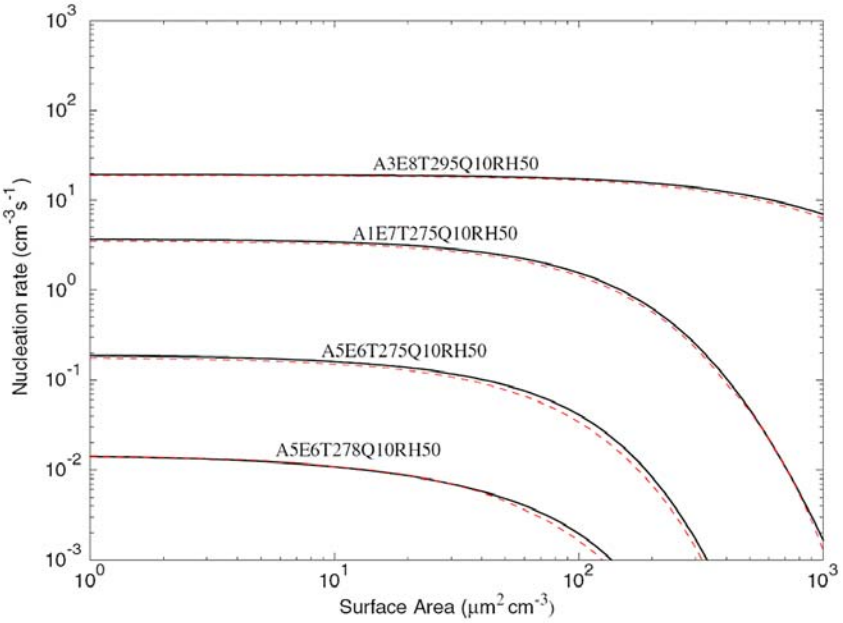

Figure 5. The dependence of predicted IMN rates on S under four selected conditions, based on the full IMN model (solid lines) and IMN look-up table (dashed lines). In the legend, read A1E7T275Q10RH50 as $[H_2SO_4] = 3 \times 10^7 cm^{-3}$, Q = 10 ion pairs $cm^{-3}s^{-1}$, T = 275 K, and RH = 50%.

be simplified to reduce computing costs. In the past, various versions of parameterizations have been derived for binary, ternary, and ion nucleation. The parameterization formulas become complex and very lengthy as the number of parameters determining nucleation rates increases [*Modgil et al.*, 2005]. Furthermore, it is hard to obtain accurate parameterization for all the possible ranges of input parameters. For example, the ion nucleation rates calculated with the parameterization of *Modgil et al.* [2005] can deviate by more than 1 order of magnitude from those calculated by the nucleation model under some parameter spaces.

[35] *Yu* [2008] developed an alternative approach, look-up tables, to reduce the computing costs for 3-D nucleation rate calculations. With the pregenerated look-up table and a simple interpolation subroutine, nucleation rates under given conditions can be calculated accurately (compared to the results from full model simulation) and efficiently. One advantage of the look-up table is that it can cover any needed variable ranges and provide nucleation rates with good accuracy for all the parameter spaces. Another advantage is that it is capable of handling five or more input variables, which is difficult to obtain via parameterizations.

[36] Here we describe the look-up table of steady state ion-mediated nucleation rates under a wide range of atmospheric conditions. The table is derived by running an updated version of the kinetic IMN model. The tabulated ion-mediated nucleation rates (J_{IMN}) depend on $[H_2SO_4]$, RH, T, Q, and S, and thus the look-up table is five-dimensional. The number of sulfuric acid molecules in the critical cluster (n_a*), the acid mole fraction (AMOLF*, defined as the relative mole fraction of H_2SO_4 in the system of H_2SO_4 and H_2O), and diameter (d*) of the critical cluster are also included in the look-up table.

[37] Table 1 shows the range of each dependent variable dimension, total number of points in each dimension, and values at each point for the look-up table. In the IMN look-up table, T ranges from 190 K to 302 K with a resolution of 2 K and RH ranges from 0.5% to 99.5% with a resolution of 2%. $[H_2SO_4]$ ranges from $5 \times 10^5 - 5 \times 10^8$ cm^{-3} with a resolution of 10 values per decade (geometric), Q ranges from 1.5 to 60 ion pairs $cm^{-3}s^{-1}$ with a resolution of 5 values per decade (geometric), and S ranges from 10 to

Table 1. Range of Each Dependent Variable Dimension, Total Number of Points in Each Dimension, and Values at Each Point for the IMN Look-Up Table

	Range	Total Number of Points	Values at Each Point
$[H_2SO_4]$ (cm^{-3})	(5×10^5)–(5×10^8)	31	$[H_2SO_4](i) = 5 \times 10^5 \times 10^{(i-1)/10}$, i = 1, 31
T (K)	190–302	57	$T(j) = 190 + 2 \times (j - 1)$, j = 1, 57
RH (%)	0.5–99.5	51	RH(1) = 0.5, $RH(k) = 2 \times (k-1)$, k = 2, 50; RH(51) = 99.5
Q (ion pairs $cm^{-3}s^{-1}$)	1.5–60	9	$Q(l) = 1.5 \times 10^{(l-1)/5}$, l = 1, 9
S ($\mu m^2 cm^{-3}$)	1–1000	7	$S(1) = 1$, $S(m) = 10 \times 10^{(m-2)/2.5}$, m = 2, 7

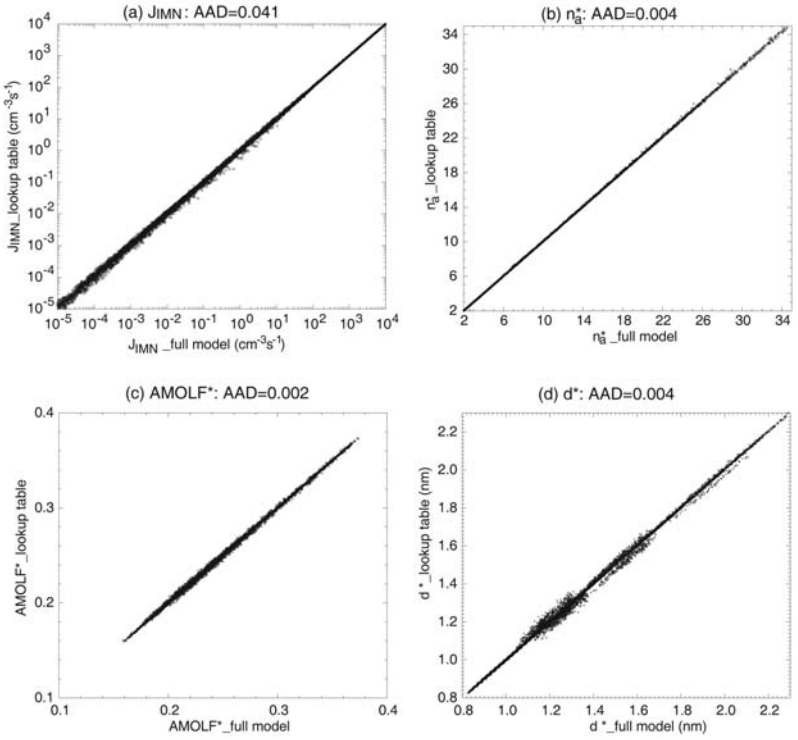

Figure 6. Comparisons of (a) J_{IMN}, (b) n_a*, (c) AMOLF*, and (d) d* interpolated from the IMN look-up table with those calculated with full IMN model. See text for the definition of the average absolute deviations (AAD) given in each plot.

1000 $\mu m^2 cm^{-3}$ with a resolution of 2.5 values per decade (geometric) plus one point at S = 1 $\mu m^2 cm^{-3}$. These parameter ranges should cover almost all the possible conditions in the troposphere relevant to atmospheric nucleation. The range and resolution in each parameter space can be extended in the future if needed. The look-up table is composed of J, n_a*, AMOLF*, and d* values at $31 \times 57 \times 51 \times 9 \times 7 = 5{,}677{,}371$ points, and has a total size of ~50 MB in the text format. The look-up table, along with a FORTRAN code to read and interpolate the tables, is given in the AGU auxiliary material.[1] For quick application, one can obtain J_{IMN} using an online nucleation rate calculator (http://www.albany.edu/~yfq/YuOnLineNucleation.html) developed by the author.

[38] For any given values of $[H_2SO_4]$, T, RH, Q, and S within the ranges specified in Table 1, J_{IMN} and properties of critical clusters (n_a*, AMOLF*, and d*) can be obtained using the look-up table with an efficient multiple-variable interpolation scheme described in Appendix A. In Figures 1–5, the values of J_{IMN} interpolated from the look-up table (J_{IMN}^{LT}) are plotted along with those calculated with the full model (J_{IMN}^{FM}) and we can see that J_{IMN}^{LT} is very close to J_{IMN}^{FM} under the shown conditions. To explore the accuracy of the interpolated values under other conditions, we randomly generated 30,000 combinations of $[H_2SO_4]$, T, RH, Q, and S within the specified ranges. It should be noted that many of those combinations are very unlikely to happen in the atmosphere. J_{IMN} is between 10^{-5} and 10^4 $cm^{-3}s^{-1}$ in about 18,000 out of these 30,000 conditions. A comparison of J_{IMN}, n_a*, AMOLF*, and d* interpolated from the look-up table (LT) with those calculated with full model (FM) are given in Figure 6. The average absolute deviations (AAD) marked in each plot are defined as

$$\mathrm{AAD} = \frac{\sum_1^N \left| \frac{X^{LT} - X^{FM}}{X^{FM}} \right|}{N},$$

where X = J_{IMN}, n_a*, AMOLF*, and d* and N is the total numbers of cases with J_{IMN} between 10^{-5} and 10^4 $cm^{-3}s^{-1}$.

[39] It is clear from Figure 6 that the differences between the interpolated values and those corresponding values calculated with full IMN model are generally within a few percentages (AAD $\leq$ ~4%). The cases with relatively large deviations are those cases falling into the parameter spaces where nucleation rates are sensitive to the changes in the parameters (i.e., the steepest part of curves shown in Figures 1–5). The deviations can be reduced if we increase the resolution of the look-up table. Considering the current uncertainty in the IMN model [*Yu*, 2006], we think that the results from the present look-up table are acceptable.

[40] The application of the look-up table significantly reduces the computing time needed to calculate large

[1] Auxiliary materials are available in the HTML. doi:10.1029/2009JD012630.

numbers of IMN rates, such as required in three-dimensional modeling. In a UNIX workstation we tested, it takes about 0.3 s CPU time to calculate J_{IMN}, n_a*, AMOLF*, and d* for 30,000 randomly selected cases using the look-up table while it takes about 2350 s CPU time when we use the full IMN model. Thus, the look-up table reduces the computing time by a factor of ~8000. The IMN look-up table has been successfully incorporated into a global chemical transport model [*Yu et al.*, 2008; *Yu and Luo*, 2009] and the nucleation rate calculation has a very small effect on the overall global simulation computing time.

5. Summary

[41] The primary mechanisms of particle nucleation, which control aerosol number concentrations to a significant degree, remain elusive, despite decades of intensive study. An ion-mediated nucleation (IMN) mechanism based on a kinetic model, which incorporates new thermodynamic data and physical algorithms and explicitly treats the evaporation of neutral and charged clusters, is supported by long-term measurements of cluster ion spectrum evolution during nucleation events and the excess charge on freshly nucleated particles. With the kinetic IMN model that explicitly resolves the size-dependent microphysical processes among precursor gases and charged and neutral clusters/particles ranging from molecular sizes to several micrometers, we systematically investigate the key parameters controlling IMN rate (J_{IMN}).

[42] We show that sulfuric acid vapor concentration ($[H_2SO_4]$), temperature (T), relative humidity (RH), ionization rate (Q), and surface area of preexisting particles (S) have profound and nonlinear impacts on J_{IMN}. Generally, J_{IMN} is larger when $[H_2SO_4]$ and RH are higher, and T and S are lower. J_{IMN} generally increases with Q unless Q is large and $[H_2SO_4]$ is relatively small. With other parameters fixed, J_{IMN} may be insensitive to some parameters under certain conditions when J_{IMN} is limited by other parameter(s). According to the IMN mechanism, T and $[H_2SO_4]$ are the two most important factors controlling the start and end of nucleation events, although other parameters also contribute to the changes in nucleation rates. The implications of such dependences are discussed. The critical impact of T and $[H_2SO_4]$ on J_{IMN} may explain the general occurrence of nucleation in the morning hours and peak of nucleation frequency in the Spring and Fall. More importantly, systematic changes in T and $[H_2SO_4]$ associated with future climate and emission changes may substantially affect nucleation rates and aerosol indirect radiative forcing and thus may imply important climate feedback mechanisms. In addition, the dependence of J_{IMN} on ionization rates may provide a physical mechanism amplifying the effect of solar variations on Earth's climate.

[43] An IMN look-up table derived using the most recent version of the IMN model is presented. The look-up table is five-dimensional with the key parameters covering almost all the tropospheric conditions relevant to atmospheric nucleation. With the look-up table and a multiple-variable interpolation subroutine, one can calculate the IMN rates and the properties of critical clusters under given conditions efficiently and accurately. The usage of the look-up table reduces the computational costs of the IMN rate calculations by a factor of ~8000 and requires negligible computing resources in multidimensional simulations.

Appendix A: Multivariable Linear Interpolation Scheme

[44] The tabulated ion-mediated nucleation rates (J_{IMN}) depend on $[H_2SO_4]$, RH, T, Q, and S, and thus the look-up table is five-dimensional. The properties of critical clusters (n_a*, AMOLF*, and d*) depend on $[H_2SO_4]$, RH, and T, and thus the corresponding look-up table is three-dimensional. For any set of $[H_2SO_4]$, RH, T, Q, and S, J_{IMN} along with n_a*, AMOLF*, and d* can be calculated efficiently based on a multiple-variable linear interpolation scheme described below. We use J_{IMN} as an example.

[45] Let $x = [H_2SO_4]$, $y = RH$, $z = T$, $u = Q$, $v = S$, and $J = J_{IMN}$, then $J = f(x, y, z, u, v)$. To find J_0 value at the point $(x_0, y_0, z_0, u_0, v_0)$, we first need to locate the closest set of grid points surrounding the point $(x_0, y_0, z_0, u_0, v_0)$ in each look-up table dimension: $x_1 \le x_0 < x_2$; $y_1 \le y_0 < y_2$; $z_1 \le z_0 < z_2$; $u_1 \le u_0 < u_2$; $v_1 \le v_0 < v_2$. The values of points of look-up table given in Table 1 are designed in a way that x_1, x_2, y_1, y_2, z_1, z_2, u_1, u_2, v_1, and v_2 can be determined quickly with a simple calculation (based on the analytical formula given in the last column of Table 1).

A1. Linear Interpolation: J = f(x)

[46] Let $J_1 = f(x_1)$, $J_2 = f(x_2)$, and $dx = x_2 - x_1$, $dx_1 = x_0 - x_1$, $dx_2 = x_2 - x_0$, then

$$J_0 = f(x_0) = J_1 + (J_2 - J_1)dx_1/dx = (J_1 dx_2 + J_2 dx_1)/dx \quad \text{(A1)}$$

A2. Bilinear Interpolation: J = f(x, y)

[47] For any given point (x_0, y_0), there are $2^2 = 4$ surrounding points. Let $J_{11} = f(x_1, y_1)$, $J_{12} = f(x_1, y_2)$, $J_{21} = f(x_2, y_1)$, $J_{22} = f(x_2, y_2)$, $dy = y_2 - y_1$, $dy_1 = y_0 - y_1$, $dy_2 = y_2 - y_0$.

[48] First, obtain J_{10} and J_{20} based on linear interpolation (equation (A1)),

$$J_{10} = f(x_1, y_0) = (J_{11}dy_2 + J_{12}dy_1)/dy$$

$$J_{20} = f(x_2, y_0) = (J_{21}dy_2 + J_{22}dy_1)/dy$$

Then use linear interpolation (equation (A1)) again to get

$$\begin{aligned} J_{00} &= f(x_0, y_0) = (J_{10}dx_2 + J_{20}dx_1)/dx \\ &= (J_{11}dx_2dy_2 + J_{12}dx_2dy_1 + J_{21}dx_1dy_2 + J_{22}dx_1dy_1)/(dxdy). \end{aligned} \quad \text{(A2)}$$

A3. Trilinear Interpolation: J = f(x, y, z)

[49] For any given point (x_0, y_0, z_0), there are $2^3 = 8$ surrounding points. Let $J_{111} = f(x_1, y_1, z_1)$, $J_{112} = f(x_1, y_1, z_2)$, ..., $J_{221} = f(x_2, y_2, z_1)$, $J_{222} = f(x_2, y_2, z_2)$, $dz = z_2 - z_1$, $dz_1 = z_0 - z_1$, $dz_2 = z_2 - z_0$. We can get $J_{000} = (x_0, y_0, z_0)$ by reducing the trilinear interpolation to bilinear interpolation.

[50] First, get J_{110}, J_{120}, J_{210}, J_{220} based on equation (A1),

$$J_{110} = f(x_1, y_1, z_0) = (J_{111}dz_2 + J_{112}dz_1)/dz,$$

$$J_{120} = f(x_1, y_2, z_0) = (J_{121}dz_2 + J_{122}dz_1)/dz,$$

$$J_{210} = f(x_2, y_1, z_0) = (J_{211}dz_2 + J_{212}dz_1)/dz,$$

$$J_{220} = f(x_2, y_2, z_0) = (J_{221}dz_2 + J_{222}dz_1)/dz.$$

Then, obtain $J_{000} = (x_0, y_0, z_0)$ with equation (A2),

$$J_{000} = (J_{111}dx_2dy_2dz_2 + J_{112}dx_2dy_2dz_1 + \ldots J_{221}dx_1dy_1dz_2 + J_{222}dx_1dy_1dz_1)/(dxdydz). \quad (A3)$$

A4. Multivariable Linear Interpolation

[51] The above derivation of linear interpolation can be generalized to a system with N variables. The strategy is to reduce the number of variables by 1 with equation (A1), and then apply (N-1) linear interpolation formula to get the final interpolation expression.

[52] For the 5-D look-up table J = f(x, y, z, u, v), there are $2^5 = 32$ grid points surrounding any given point (x_0, y_0, z_0, y_0, z_0). The formula for determining $J_{00000} = f(x_0, y_0, z_0, u_0, v_0)$ can be expressed as

$$J_{00000} = (J_{11111}dx_2dy_2dz_2du_2dv_2 + J_{11112}dx_2dy_2dz_2du_2dv_1 + \ldots J_{22221}dx_1dy_1dz_1du_1dv_2 + J_{22222}dx_1dy_1dz_1du_1dv_1)/(dxdydzdudv), \quad (A4)$$

where $J_{11111} = f(x_1, y_1, z_1, u_1, v_1)$, $J_{11112} = f(x_1, y_1, z_1, u_1, v_2)$, . . ., $J_{22221} = f(x_2, y_2, z_2, u_2, v_1)$, $J_{22222} = f(x_2, y_2, z_2, u_2, v_2)$, $du = u_2 - u_1$, $du_1 = u_0 - u_1$, $du_2 = u_2 - u_0$, $dv = v_2 - v_1$, $dv_1 = v_0 - v_1$, $dv_2 = v_2 - v_0$.

[53] **Acknowledgments.** This study is supported by NSF under grant 0618124, NASA under grant NNX08AK48G, and NOAA under grant NA05OAR4310103.

References

Albrecht, B. A. (1989), Aerosols, cloud microphysics and fractional cloudiness, *Science*, *245*, 1227–1230.

Arnold, F. (1980), Multi-ion complexes in the stratosphere—Implications for trace gases and aerosol, *Nature*, *284*, 610–611, doi:10.1038/284610a0.

Boy, M., J. Kazil, E. R. Lovejoy, A. Guenther, and M. Kulmala (2008), Relevance of ion-induced nucleation of sulfuric acid and water in the lower troposphere over the boreal forest at northern latitudes, *Atmos. Res.*, *90*, 151–158, doi:10.1016/j.atmosres.2008.01.002.

Carter, P. J., and G. B. Johnson (1988), Space charge measurements downwind from a monopolar 500 kV HVDC test line, *IEEE Trans. Power Delivery*, *3*, 2056–2063, doi:10.1109/61.194017.

Castleman, A. W., Jr., P. M. Holland, and R. G. Keesee (1978), The properties of ion clusters and their relationship to heteromolecular nucleation, *J. Chem. Phys.*, *68*, 1760–1767, doi:10.1063/1.435946.

Chan, L. Y., and V. A. Mohnen (1980), The formation of ultrafine ion H_2O-H_2SO_4 aerosol particles through ion-induced nucleation process in the stratosphere, *J. Aerosol Sci.*, *11*, 35–45, doi:10.1016/0021-8502(80)90142-1.

Charlson, R. J., J. E. Lovelock, M. O. Andreae, and S. G. Warren (1987), Oceanic phytoplankton, atmospheric sulphur, cloud albedo and climate, *Nature*, *326*, 655–661, doi:10.1038/326655a0.

Dhanorkar, S., and A. K. Kamra (1994), Diurnal variation of ionization rate close to ground, *J. Geophys. Res.*, *99*, 18,523–18,526, doi:10.1029/94JD01335.

Eisele, F. L., E. R. Lovejoy, E. Kosciuch, K. F. Moore, R. L. Mauldin III, J. N. Smith, P. H. McMurry, and K. Iida (2006), Negative atmospheric ions and their potential role in ion-induced nucleation, *J. Geophys. Res.*, *111*, D04305, doi:10.1029/2005JD006568.

Froyd, K. D. (2002), Ion induced nucleation in the atmosphere: Studies of NH_3, H_2SO_4, and H_2O cluster ions, Ph.D. thesis, Univ. of Colo. at Boulder, Boulder.

Gagné, S., L. Laakso, T. Petäjä, V.-M. Kerminen, and M. Kulmala (2008), Analysis of one year of Ion-DMPS data from the SMEAR II station, Finland, *Tellus, Ser. B*, *60*, 318–329.

Hamill, P., R. P. Turco, C. S. Kiang, O. B. Toon, and R. C. Whitten (1982), An analysis of various nucleation mechanisms for sulfate particles in the stratosphere, *J. Aerosol Sci.*, *13*, 561–585, doi:10.1016/0021-8502(82)90021-0.

Hirsikko, A., et al. (2007), Identification and classification of the formation of intermediate ions measured in boreal forest, *Atmos. Chem. Phys.*, *7*, 201–210.

Iida, K., M. Stolzenburg, P. McMurry, M. J. Dunn, J. N. Smith, F. Eisele, and P. Keady (2006), Contribution of ion-induced nucleation to new particle formation: Methodology and its application to atmospheric observations in Boulder, Colorado, *J. Geophys. Res.*, *111*, D23201, doi:10.1029/2006JD007167.

Intergovernmental Panel on Climate Change (2007), *Climate Change 2007: The Physical Scientific Basis*, edited by S. Solomon et al., Cambridge Univ. Press, New York.

Kazil, J., and E. R. Lovejoy (2007), A semi-analytical method for calculating rates of new sulfate aerosol formation from the gas phase, *Atmos. Chem. Phys.*, *7*, 3447–3459.

Kulmala, M., et al. (2004a), Formation and growth rates of ultrafine atmospheric particles: A review of observations, *J. Aerosol Sci.*, *35*, 143–176, doi:10.1016/j.jaerosci.2003.10.003.

Kulmala, M., et al. (2004b), Initial steps of aerosol growth, *Atmos. Chem. Phys.*, *4*, 2553–2560.

Kulmala, M., et al. (2007), Toward direct measurement of atmospheric nucleation, *Science*, *318*, 89–92, doi:10.1126/science.1144124.

Laakso, L., J. M. Mäkelä, L. Pirjola, and M. Kulmala (2002), Model studies of ion-induced nucleation in the atmosphere, *J. Geophys. Res.*, *107*(D20), 4427, doi:10.1029/2002JD002140.

Laakso, L., et al. (2007), Detecting charging state of ultra-fine particles: Instrumental development and ambient measurements, *Atmos. Chem. Phys.*, *7*, 1333–1345.

Laaksonen, A., et al. (2008), The role of VOC oxidation products in continental new particle formation, *Atmos. Chem. Phys.*, *8*, 2657–2665.

Lovejoy, E. R., J. Curtius, and K. D. Froyd (2004), Atmospheric ion-induced nucleation of sulfuric acid and water, *J. Geophys. Res.*, *109*, D08204, doi:10.1029/2003JD004460.

Manninen, H. E., et al. (2009), Charged and total particle formation and growth rates during EUCAARI 2007 campaign in Hyytiälä, *Atmos. Chem. Phys. Discuss.*, *9*, 5119–5151.

McMurry, P. H., et al. (2005), A criterion for new particle formation in the sulfur-rich Atlanta atmosphere, *J. Geophys. Res.*, *110*, D22S02, doi:10.1029/2005JD005901.

Minschwaner, K., and A. E. Dessler (2004), Water vapor feedback in the tropical upper troposphere: Model results and observations, *J. Clim.*, *17*, 1272–1282, doi:10.1175/1520-0442(2004)017<1272:WVFITT>2.0.CO;2.

Modgil, M. S., S. Kumar, S. N. Tripathi, and E. R. Lovejoy (2005), A parameterization of ion-induced nucleation of sulphuric acid and water for atmospheric conditions, *J. Geophys. Res.*, *110*, D19205, doi:10.1029/2004JD005475.

Nadykto, A., and F. Yu (2003), Uptake of neutral polar vapor molecules by charged particles: Enhancement due to dipole-charge interaction, *J. Geophys. Res.*, *108*(D23), 4717, doi:10.1029/2003JD003664.

Ney, E. P. (1959), Cosmic radiation and the weather, *Nature*, *183*, 451–452, doi:10.1038/183451a0.

O'Dowd, C. D., et al. (2008), Airborne measurements of nucleation mode particles II: Boreal forest nucleation events, *Atmos. Chem. Phys. Discuss.*, *8*, 2821–2848.

Raes, F., J. Augustin, and R. Vandingenen (1986), The role of ion-induced aerosol formation in the lower atmosphere, *J. Aerosol Sci.*, *17*, 466–470, doi:10.1016/0021-8502(86)90135-7.

Reiter, R. (1992), *Phenomena in Atmospheric and Environmental Electricity*, Elsevier, New York.

Stanier, C., A. Khlystov, and S. N. Pandis (2004), Nucleation events during the Pittsburgh Air Quality Study: Description and relation to key meteorological, gas phase, and aerosol parameters, *Aerosol Sci. Technol.*, *38*(suppl. 1), 253–264, doi:10.1080/02786820390229570.

Suda, T., and Y. Sunaga (1990), An experimental study of large ion density under the Shiobara HVDC test line, *IEEE Trans. Power Delivery*, *5*, 1426–1435, doi:10.1109/61.57985.

Twomey, S. (1977), The influence of pollution on the shortwave albedo of clouds, *J. Atmos. Sci.*, *34*, 1149–1152, doi:10.1175/1520-0469(1977)034<1149:TIOPOT>2.0.CO;2.

Vartiainen, E., et al. (2007), Ion and particle number concentrations and size distributions along the Trans-Siberian railroad, *Boreal Environ. Res.*, *12*, 375–396.

Wilhelm, S., S. Eichkorn, D. Wiedner, L. Pirjola, and F. Arnold (2004), Ion-induced aerosol formation: New insights from laboratory measurements of mixed cluster ions, HSO_4^- $(H_2SO_4)_a$ $(H_2O)_w$ and H^+ $(H_2SO_4)_a$ $(H_2O)_w$, *Atmos. Environ.*, *38*, 1735–1744, doi:10.1016/j.atmosenv.2003.12.025.

Yu, F. (2002), Altitude variations of cosmic ray induced production of aerosols: Implications for global cloudiness and climate, *J. Geophys. Res.*, *107*(A7), 1118, doi:10.1029/2001JA000248.

Yu, F. (2005), Modified Kelvin-Thomson equation considering ion-dipole interaction: Comparison with observed ion-clustering enthalpies and entropies, *J. Chem. Phys.*, *122*, 084503, doi:10.1063/1.1845395.

Yu, F. (2006), From molecular clusters to nanoparticles: Second-generation ion-mediated nucleation model, *Atmos. Chem. Phys.*, *6*, 5193–5211.

Yu, F. (2007), An improved quasi-unary nucleation model for binary H_2SO_4-H_2O homogeneous nucleation, *J. Chem. Phys.*, *127*, 054301, doi:10.1063/1.2752171.

Yu, F. (2008), Updated H_2SO_4-H_2O binary homogeneous nucleation rate look-up tables, *J. Geophys. Res.*, *113*, D24201, doi:10.1029/2008JD010527.

Yu, F., and G. Luo (2009), Simulation of particle size distribution with a global aerosol model: Contribution of nucleation to aerosol and CCN number concentrations, *Atmos. Chem. Phys.*, *9*, 7691–7710.

Yu, F., and R. P. Turco (1997), The role of ions in the formation and evolution of particles in aircraft plumes, *Geophys. Res. Lett.*, *24*, 1927–1930, doi:10.1029/97GL01822.

Yu, F., and R. P. Turco (2000), Ultrafine aerosol formation via ion-mediated nucleation, *Geophys. Res. Lett.*, *27*, 883–886, doi:10.1029/1999GL011151.

Yu, F., and R. P. Turco (2001), From molecular clusters to nanoparticles: The role of ambient ionization in tropospheric aerosol formation, *J. Geophys. Res.*, *106*, 4797–4814, doi:10.1029/2000JD900539.

Yu, F., and R. P. Turco (2007), Charging state of freshly nucleated particles: Implication for nucleation mechanisms, in *Nucleation and Atmospheric Aerosols*, edited by C. D. O'Dowd and P. E. Wagner, pp. 392–396, Springer, New York.

Yu, F., and R. P. Turco (2008), Case studies of particle formation events observed in boreal forests: Implications for nucleation mechanisms, *Atmos. Chem. Phys.*, *8*, 6085–6102.

Yu, F., et al. (2007), Interactive comment on "Ion-mediated nucleation as an important global source of tropospheric aerosols", *Atmos. Chem. Phys. Discuss.*, *7*, S6602–S6608, www.atmos-chem-phys-discuss.net/7/S6602/2007.

Yu, F., Z. Wang, G. Luo, and R. P. Turco (2008), Ion-mediated nucleation as an important source of tropospheric aerosols, *Atmos. Chem. Phys.*, *8*, 2537–2554.

F. Yu, Atmospheric Sciences Research Center, State University of New York at Albany, 251 Fuller Rd., Albany, NY 12203, USA. (yfq@asrc.cestm.albany.edu)